Inorganic Chemistry

pubs.acs.org/IC Article

Spin-Lattice Coupling Across the Magnetic Quantum-Phase Transition in Copper-Containing Coordination Polymers

Kendall D. Hughey, Nathan C. Harms, Kenneth R. O'Neal, Amanda J. Clune, Jeffrey C. Monroe, Avery L. Blockmon, Christopher P. Landee, Zhenxian Liu, Mykhaylo Ozerov, and Janice L. Musfeldt*



Cite This: Inorg. Chem. 2020, 59, 2127–2135



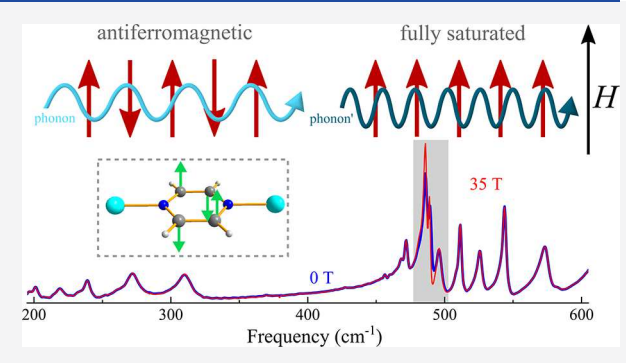
ACCESS

III Metrics & More

Article Recommendations

Supporting Information

ABSTRACT: We measured the infrared vibrational properties of two copper-containing coordination polymers, $[Cu(pyz)_2(2-HOpy)_2]-(PF_6)_2$ and $[Cu(pyz)_{1.5}(4-HOpy)_2](ClO_4)_2$, under different external stimuli in order to explore the microscopic aspects of spin—lattice coupling. While the temperature and pressure control hydrogen bonding, an applied field drives these materials from the antiferromagnetic \rightarrow fully saturated state. Analysis of the pyrazine (pyz)-related vibrational modes across the magnetic quantum-phase transition provides a superb local probe of magnetoelastic coupling because the pyz ligand functions as the primary exchange pathway and is present in both systems. Strikingly, the PF₆⁻ compound employs several pyz-related distortions in support of the magnetically driven



transition, whereas the ClO_4^- system requires only a single out-of-plane pyz bending mode. Bringing these findings together with magnetoinfrared spectra from other copper complexes reveals spin—lattice coupling across the magnetic quantum-phase transition as a function of the structural and magnetic dimensionality. Coupling is maximized in $[Cu(pyz)_{1.5}(4-HOpy)_2](ClO_4)_2$ because of its ladderlike character. Although spin—lattice interactions can also be explored under compression, differences in the local structure and dimensionality drive these materials to unique high-pressure phases. Symmetry analysis suggests that the high-pressure phase of the ClO_4^- compound may be ferroelectric.

INTRODUCTION

Molecule-based materials offer fascinating opportunities to investigate the interplay between the structure and magnetism.1-8 Soft ligands, which link the metal centers and introduce characteristically low-energy scales and flexible architectures, are crucial to driving new quantum phases and exciting functionality. 9-13 Copper-containing coordination polymers are outstanding platforms with which to explore these ideas. They sport low-dimensional quantum $(S = \frac{1}{2})$ behavior, strong hydrogen and halogen bonds that act as exchange pathways, and magnetic quantum-phase transitions at experimentally realizable fields that emanate from the overall low-magnetic-energy scales. 14-19 Quantum-phase transitions are different from classical phase transitions in that they are driven by a physical tuning parameter like magnetic field, composition, or pressure and governed by quantum (rather than by thermal) fluctuations. 12,14,20-22 Those involving an applied field are the most well studied. Because of their lowenergy scales, copper-containing quantum magnets also provide a platform for unraveling some of the properties of high-temperature copper oxides. ^{23,24} These materials crystallize in a variety of patterns and dimensionalities, ranging from zerodimensional systems to three-dimensional networks. 2,25-27 Although scaling and fluctuation physics in low-dimensional

magnetic materials have been investigated, ^{28,29} other interactions and trends have not received the same attention, likely because of the lack of a progression of materials in the same family. For instance, spin—lattice coupling across a magnetic quantum-phase transition and the structure—property relations that emerge are highly underexplored. Furthermore, very few of these studies extend toward high-pressure phases, despite the well-known lattice flexibility and accessible compression-induced transitions. ^{25,30–32} [Cu(pyz)₂(2-HOpy)₂](PF₆)₂ and [Cu(pyz)_{1.5}(4-HOpy)₂](ClO₄)₂ attracted our attention in this regard.

 $[Cu(pyz)_2(2-HOpy)_2](PF_6)_2$ is a highly isolated two-dimensional $S={}^1/_2$ Heisenberg antiferromagnet. The Cu^{2+} centers are six-coordinated and linked via pyrazine (pyz) ligands in the ab plane to create an infinitely extending, two-dimensional square lattice. These layers are stabilized along the c axis via hydrogen-bonding interactions from pyridone (py) ligands to uncoordinated PF_6^- anions (Figure 1a). 33

Received: August 7, 2019 Published: February 3, 2020



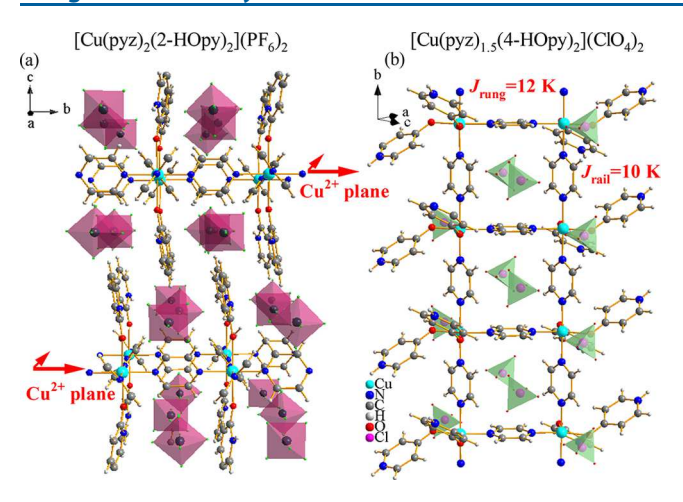


Figure 1. (a) Crystal structure of $[Cu(pyz)_2(2-HOpy)_2](PF_6)_2$ emphasizing the layered, infinitely extending Cu^{2+} planes. (b) View of the ladder structure $[Cu(pyz)_{1.5}(4-HOpy)_2](ClO_4)_2$. Exchange strengths of the rung versus rail are indicated.^{35,34}

Antiferromagnetism develops below $T_{\rm N}=1.37$ K, and the intralayer exchange strength is 6.8 K. The latter corresponds to a magnetic saturation field of 19 T.³³ Although two-dimensional magnetism is (in general) well-studied,⁷ the large layer isolation in $[{\rm Cu(pyz)_2(2-HOpy)_2}]({\rm PF_6})_2$ sets it apart.^{35,36}

The structure of $[Cu(pyz)_{1.5}(4-HOpy)_2](ClO_4)_2$ is quite different.³⁴ In this material, the Cu²⁺ centers are coupled through pyz ligands along the a and b axes. Here, Cu^{2+} is fivecoordinated, and py serves as a capping ligand for the metal centers. They are stabilized in a staggered formation by hydrogen bonds to semicoordinated perchlorate (ClO₄⁻) groups (Figure 1b). Thus, the system is a spin ladder in which long-range Cu···Cu interactions are oriented along the b axis but do not extend in other directions. Instead, hydrogenbonding interactions hold the ladders together. Susceptibility measurements give exchange interactions of $J_{\rm rung} = 10.4$ K and $J_{\rm rail} = 12$ K, resulting in $J_{\rm rung}/J_{\rm rail} = 0.87-$ very close to an isotropic value.³⁴ This material bridges an important gap in the field of low-dimensional magnetism by providing a physical realization of a spin-ladder system with modest energy scales and $J_{\text{rung}}/J_{\text{rail}}$ close to 1.0. High-field magnetization reveals a spin gap Δ of about 5 T and a 24 T saturation field $B_{\rm C}$. Table 1 summarizes these properties. Importantly, the magnetic quantum-phase transitions are accessible with currently available powered magnets. This allows exploration of the properties across B_C .

In this work, we combined infrared spectroscopy with several different physical tuning techniques to investigate spin—lattice coupling in two copper-containing coordination

Table 1. Summary of the Properties Comparing $[Cu(pyz)_2(2-HOpy)_2](PF_6)_2$ and $[Cu(pyz)_{1.5}(4-HOpy)_2](ClO_4)_2^{33,34a}$

material	$T_{N}(K)$	$_{(T)}^{\Delta}$	$B_{\rm C}$ (T)	J (K)	$P_{\rm C}$ (GPa)
$ \begin{array}{c} [\operatorname{Cu}(\operatorname{pyz})_2(2-\\ \operatorname{HOpy})_2](\operatorname{PF}_6)_2 \end{array} $	1.37		19	6.8 (<i>ab</i> -plane)	3.7 ^a
$ \begin{array}{c} \left[\text{Cu(pyz)}_{1.5} (\text{4-} \\ \text{HOpy)}_{2} (\text{ClO}_{4})_{2} \end{array} \right. $	<1.5	≈5	24	10.4 (rung); 12.0 (rail)	4.5 ^a

^aValues derived in this work.

polymers, $[Cu(pyz)_2(2-HOpy)_2](PF_6)_2$ and $[Cu(pyz)_1_5(4-Pyz)_2](PF_6)_2$ $HOpy)_2$ (ClO₄)₂. Analysis of the pyz-related vibrational modes provides a superb local probe of magnetoelastic effects because this ligand functions as the primary exchange pathway and is present in both systems. Variable-temperature and highpressure spectroscopies reveal improved hydrogen bonding in the PF₆ complex because of the natural tendency for twodimensional layers to compress. These effects are less apparent in the ClO₄ system because the important distortions are intra- rather than inter-ladder in nature. An applied field drives [Cu(pyz)₂(2-HOpy)₂](PF₆)₂ through a magnetic quantumphase transition at $B_C = 19$ T that involves several different pyz-related vibrations. In contrast, only one mode—the out-ofplane pyz distortion—is active in $[Cu(pyz)_{1.5}(4-HOpy)_2]$ -(ClO₄)₂. This is because copper dimers are less reliant on a series of local lattice distortions rather than a single displacement to facilitate the development of the fully saturated state. These findings—together with similar magnetoinfrared work on other copper complexes—are key to developing an unusual set of structure-property relationships involving both the magnetic dimensionality and spin-lattice interactions. While zero-dimensional (or "dot-like") systems connected only by intermolecular hydrogen bonds display no spin-lattice coupling across this type of field-driven transition, coupling increases in the one-dimensional case, reaches a maximum in the ladder, and falls again in layered analogues. 37-39 The availability of the intermediate dimensionality system, [Cu(pyz)_{1.5}(4-HOpy)₂](ClO₄)₂, is crucial to unveiling this trend. Unlike the coupling constant trends in a magnetic field, there are no apparent correlations under pressure. This is because the local lattice distortions across the critical pressures are much more complex than simple modifications to the Cu--pyz---Cu exchange pathway. Analysis of the candidate subgroups reveals that the ClO₄⁻ complex may be ferroelectric in the high-pressure phase, assuring future interest in this class of quantum magnets.

MATERIALS AND METHODS

Synthetic Procedures. $[Cu(pyz)_2(2-HOpy)_2](PF_6)_2$. A solution of copper dications and two hexafluorophosphate anions was prepared by dissolving 2 equiv of AgPF₆ in methanol, followed by the addition of 1 equiv of anhydrous copper chloride. Following filtration to remove the precipitated silver chloride, 2 equiv each of pyrazine (pyz) and 4-hydroxypyridine (4-HOpy) were added to the stirred filtrate. The resulting solution was partially covered and left to evaporate on a laboratory bench. After approximately a week, flat, thin green plates of $[Cu(pyz)_2(2-HOpy)_2](PF_6)_2$ appeared.³³

[Cu(pyz)₂(4-HOpy)_{1.5}](ClO₄)₂. [Cu(pyz)₂(4-HOpy)_{1.5}](ClO₄)₂ was synthesized by combining copper perchlorate hexahydrate, pyz, and 4-HOpy in a 1:2:2 molar ratio in methanol with stirring. An immediate light-blue precipitate appearred, corresponding to a pyz-bridged hydrated copper chain with the formula [Cu(pyz)(H₂O)2(4-OHpy)₂](ClO₄)₂. After filtration removed the precipitate, the medium-green filtrate was allowed to evaporate slowly, producing thin, flat blue-green crystals.³⁴

Spectroscopic Techniques. Variable-temperature infrared spectroscopy was performed using a series of Fourier transform infrared spectrometers and an open-flow cryostat system (20–5000 cm⁻¹; 4.2–300 K; 2 cm⁻¹ resolution). Absorption was calculated from the transmittance as $\alpha(\omega) = -\frac{1}{hd} \ln[\mathcal{T}(\omega)]$, where $\mathcal{T}(\omega)$ is the measured transmittance, h is the concentration, and d is the thickness. Samples were mixed with KBr or paraffin for measurements in the middle- and far-infrared regions, respectively. As discussed in the Supporting Information, we also investigated the vibrational properties of a number of chemically similar materials (Figure S1). These measure-

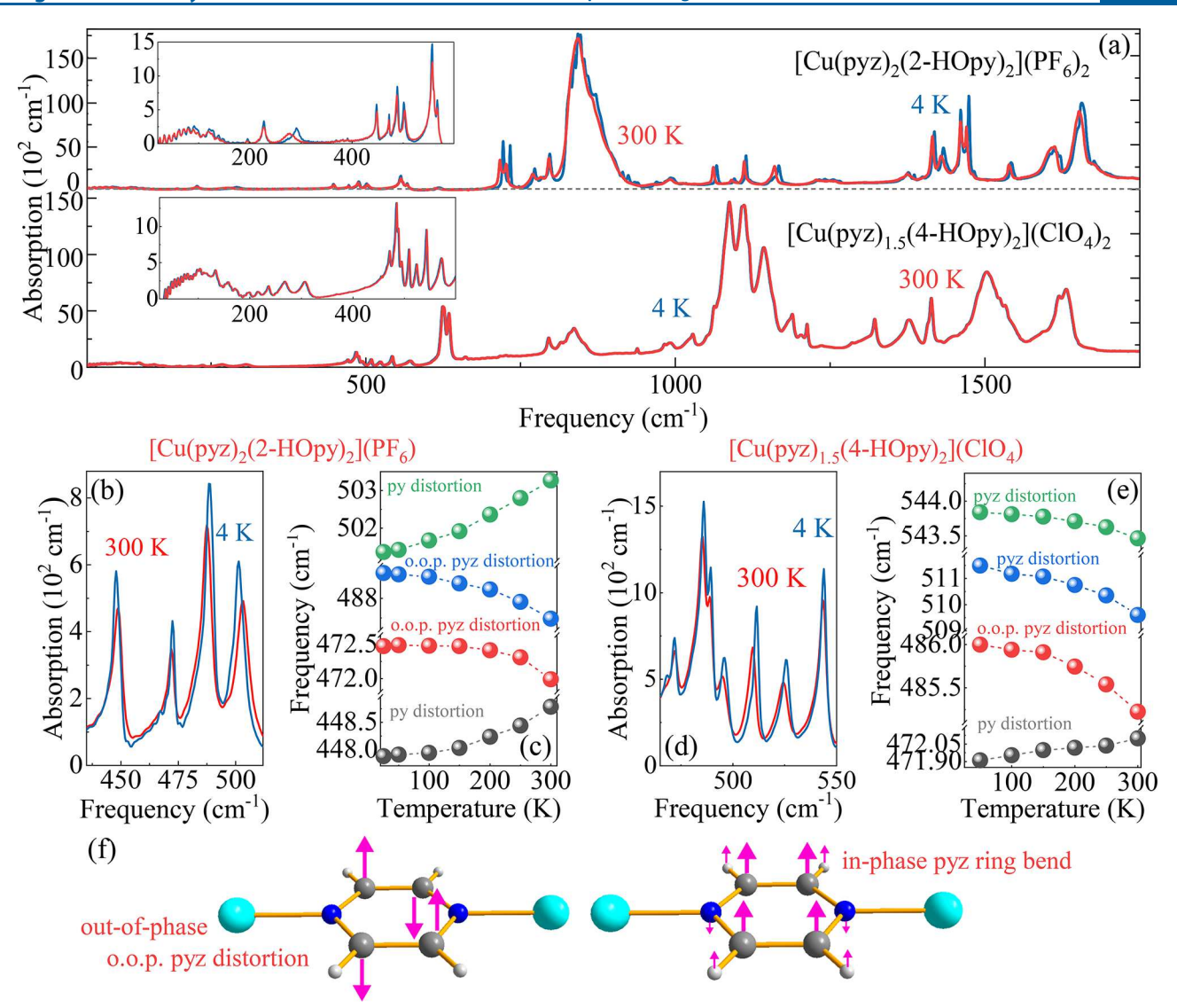


Figure 2. (a) Infrared absorption of $[Cu(pyz)_2(2\text{-HOpy})_2](PF_6)_2$ and $[Cu(pyz)_{1.5}(4\text{-HOpy})_2](ClO_4)_2$ at 300 and 4 K. Insets show the low-frequency regions. (b and c) Close-up view of the py- and pyz-containing quartet in $[Cu(pyz)_2(2\text{-HOpy})_2](PF_6)_2$ along with the corresponding peak position versus temperature trends. Specifically, we highlight the differences between hydrogen-bonded and anharmonic modes. (d and e) Close-up view of the same region in $[Cu(pyz)_{1.5}(4\text{-HOpy})_2](ClO_4)_2$. (f) Calculated displacement patterns of the out-of-plane pyz distortion and in-phase pyz ring bend.

ments, along with complementary lattice dynamics calculations, were essential for making mode assignments.

High-Field Experiments. High-field magnetoinfrared measurements were performed at the National High Magnetic Field Laboratory at 4.2 K using a 35 T resistive magnet. We present both the absorption and absorption difference, $\Delta\alpha=\alpha(\omega,B)-\alpha(\omega,B=0)$. The latter is very useful for revealing subtle spectral changes in the applied field. Using this normalized response, any deviation from a flat line implies a magnetoactive response. Because field-induced changes were quite large and signal-to-noise ratios were excellent, we also tracked the frequency as a function of the magnetic field and quantified these changes using field-induced frequency shifts: $\Delta\omega=\omega(B)-\omega(0$ T). The absorption difference and frequency shift analyses are similar. The magnetization measurements taken from refs 33 and 34 were obtained using powders. 33,34

High-Pressure Techniques. High-pressure infrared and Raman measurements (300 K; 4 cm⁻¹ resolution; 0–16 GPa) were carried out using the COMPRES beamline at the National Synchrotron Light Source II, Brookhaven National Laboratory. Samples were individually loaded into a symmetric diamond anvil cell with an annealed ruby ball. Fluorescence from an annealed ruby ball was used to determine

the pressure inside of the cell. He Because of their molecular nature, $[Cu(pyz)_2(2-HOpy)_2](PF_6)_2$ and $[Cu(pyz)_{1.5}(4-HOpy)_2](ClO_4)_2$ are very soft materials. As a result, these systems can act as their own pressure media. Our experiments were carried out with a variety of pressure media (grease, KBr, neat, etc.). For the far-infrared work shown here, we employed grease. At this level of compression (less than 10 GPa), we know the pressure to three significant figures, and the error bars on pressure due to nonhydrostatic conditions in the diamond anvil cell are on the order of the symbol size. Compression was reversible within our sensitivity. Traditional peak-fitting techniques were employed to determine frequency versus pressure trends.

RESULTS AND DISCUSSION

Development of Low-Temperature Hydrogen Bonding. Figure 2 summarizes the infrared responses of [Cu-(pyz) $_2$ (2-HOpy) $_2$](PF $_6$) $_2$ and [Cu(pyz) $_{1.5}$ (4-HOpy) $_2$](ClO $_4$) $_2$ at 300 and 4.2 K. Although the molecular aspects of this class of material yield a number of vibrational modes below 2000 cm $^{-1}$, we find that, in general, they can be divided into two

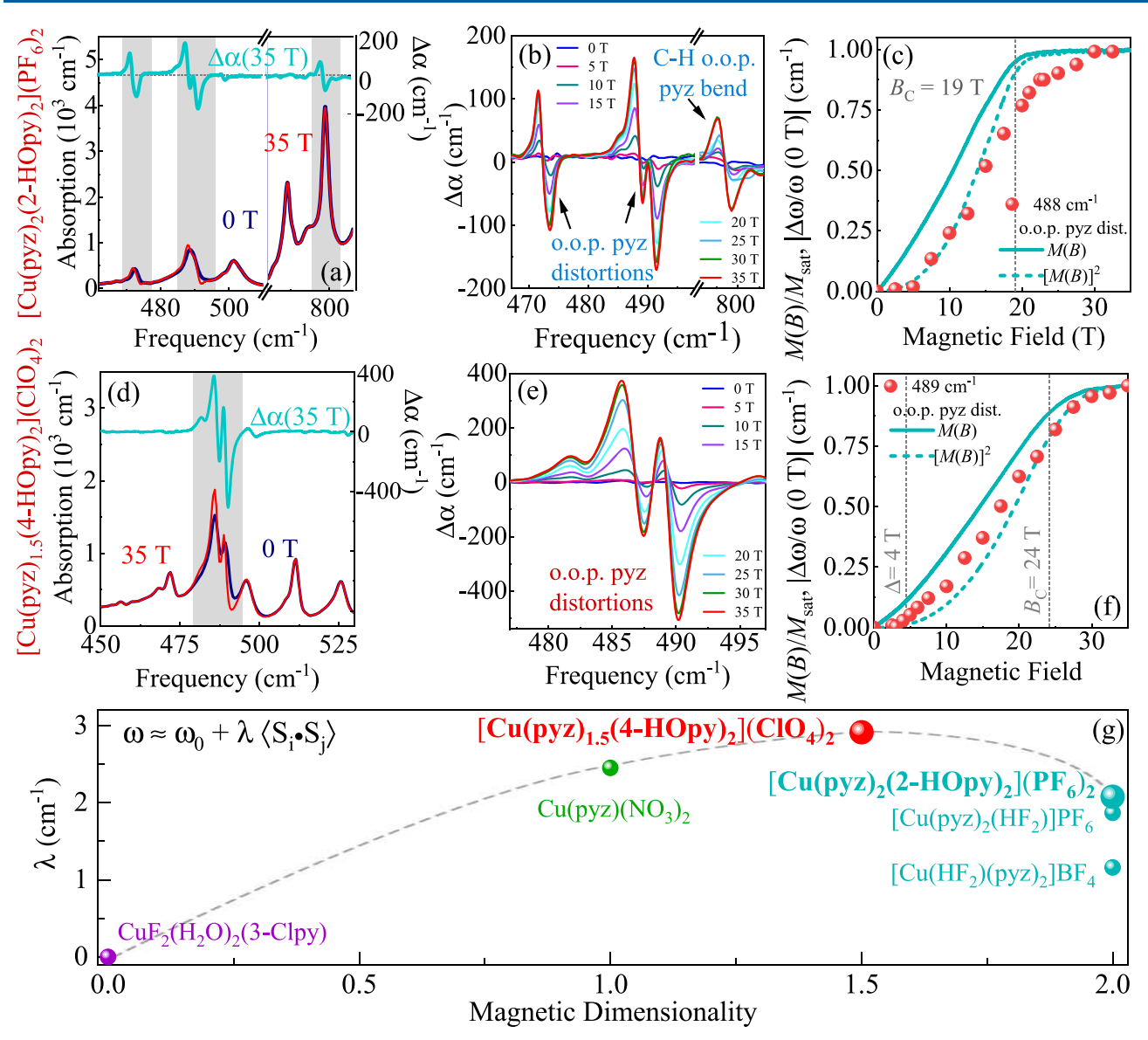


Figure 3. (a and d) Absorption (at 4.2 K) of $[Cu(pyz)_2(2-HOpy)_2](PF_6)_2$ and $[Cu(pyz)_{1.5}(4-HOpy)_2](ClO_4)_2$ at 0 and 35 T along with the 35 T absorption difference spectra. Vertical gray boxes highlight field-induced changes. (b and e) Absorption differences of the magnetoactive modes with increasing magnetic field. (c and f) Overlay of magnetic-field-induced frequency shifts of the out-of-plane pyz distortions plotted with 1.5 K magnetization 33,34 and the square of magnetization. The data sets are normalized above the critical field, B_C . (g) Comparison of the spin—phonon coupling constant of the out-of-plane pyz distortion as a function of the magnetic dimensionality in several well-known copper-containing coordination complexes. $^{37-39}$

major groups: (i) those that behave anharmonically as a function of the temperature and (ii) those that reveal characteristics of hydrogen bonding. Through dynamics calculations and comparisons with chemically analogous materials (Figure S1), 38,39,43,44 we assign the important modes. Given the fact that these materials are quite different in dimensionality and exchange strength—the PF₆⁻ complex has largely separated two-dimensional planes, whereas the ClO_4^- material is a nearly isotropic spin-ladder system—it is surprising to find that their temperature dependencies are rather similar.

In both materials, a vast majority of vibrations are pyzrelated. These ligands link the Cu^{2+} centers, forming the interplane exchanges in the two-dimensional plane as well as the rungs and rails of the ladder. These modes behave anharmonically with temperature; that is, they follow $\omega = \omega_0 + \omega_0$

 Δ (T), where Δ (T) = $C\left[1+\frac{2}{e^x-1}\right]$ with $x=\hbar\omega_0/2k_BT$, and increase in frequency with decreasing temperature. Here, ω_0 is the unperturbed phonon frequency at the base temperature, \hbar is the reduced Plank constant, and k_B is Boltzmann's constant. As examples, we highlight the modes at 472 and 488 cm⁻¹ in $\left[\text{Cu}(\text{pyz})_2(2\text{-HOpy})_2\right](\text{PF}_6)_2$, which are assigned as out-of-phase, out-of-plane pyz distortions (Figure 2c) as well as pyz-related modes above 472 cm⁻¹ in $\left[\text{Cu}(\text{pyz})_{1.5}(4\text{-HOpy})_2\right]$ - $\left(\text{ClO}_4\right)_2$ (Figure 2e).

What sets $[Cu(pyz)_2(2-HOpy)_2](PF_6)_2$ apart is that, in addition to these vibrations, we also find evidence for improved hydrogen bonding at low temperatures. This is a direct result of the separation between the layers, which are linked via relatively long hydrogen bonds from the py ligands to the PF_6^- anion via $C-H\cdots F$ interactions. With decreasing temperature, the layered material naturally contracts, allowing

hydrogen-bonding interactions to strengthen. This effect is exemplified by the 450 and 503 cm⁻¹ vibrations in Figure 2c, which characteristically redshift with decreasing temperature.⁴² Signatures of hydrogen bonding exist in the ClO₄⁻ complex as well, but the number of demonstrative vibrations are far fewer and the effects are much smaller. For instance, the out-of-plane py distortion in the ClO₄⁻ complex changes very slightly with temperature (<0.3 cm $^{-1}$), whereas in the PF $_6$ complex, changes of the same mode are on the order of 1 cm⁻¹. It is therefore clear that, in the spin ladder, although hydrogenbonding interactions connect the ladders to one another via pyz···ClO₄-···pyz pathways, the majority of the distortions occur within the rungs and rails of the individual ladders. Figure 2f displays displacement patterns of the out-of-phase, out-of-plane pyz bend along with the in-phase, out-of-plane C-H bend of the pyz. We show the latter because of the commonality of this vibration with many prominent coppercontaining complexes. 39,43 Below, we focus a majority of our discussion on the out-of-plane pyz distortions because they appear in both [Cu(pyz)₂(2-HOpy)₂](PF₆)₂ and [Cu-(pyz)_{1.5}(4-HOpy)₂](ClO₄)₂ and, as it turns out, reveal important connections to the high magnetic field and pressure-induced states.

Spin-Lattice Coupling across the Magnetic Quantum-Phase Transition. Magnetoinfrared spectroscopy provides a unique opportunity to reveal spin-lattice coupling across magnetic quantum-phase transitions in copper-containing coordination polymers and to explore how this interaction varies with the dimensionality. This is because we can compare the spectral response below and above these field-induced transitions in a variety of materials. Parts a and d of Figure 3 display the infrared absorptions of [Cu(pyz)₂(2-HOpy)₂]- $(PF_6)_2$ and $[Cu(pyz)_{1.5}(4-HOpy)_2](ClO_4)_2$ at 0 and 35 T along with the corresponding full field absorption difference spectra $\Delta \alpha(\omega) = \alpha(35 \text{ T}) - \alpha(0 \text{ T})$. The development of these features across B_C is shown with increasing magnetic field in Figure 3b,e. Although these complexes have similar chemical building blocks, the magnetoelastic interactions that facilitate the development of the fully saturated magnetic states are quite different.

In $[Cu(pyz)_2(2-HOpy)_2](PF_6)_2$, we find several fielddependent vibrational modes. These include three out-ofplane pyz distortions at 472 and 488 cm⁻¹ and a shoulder off the latter. The peak at 795 cm⁻¹, which we assign as a C-H out-of-plane pyz bend, is also active but to a lesser extent. By contrast, $[Cu(pyz)_{1.5}(4-HOpy)_2](ClO_4)_2$ displays only one field-induced feature: an out-of-plane pyz distortion, which is now a well-defined doublet at 487 and 489 cm⁻¹. These pyzrelated distortions are the only field-dependent modes; all others are rigid. This is because pyz ligands connect the Cu centers in these materials. 36,45 As a result, the out-of-plane bending mode distorts the superexchange linkage and modulates the exchange between magnetic centers. The motions of the other modes, for instance, the pyz stretch or the strongly temperature-dependent Cu-N stretch near 290 cm⁻¹, do not have the same effect on the antiferromagnetic part of J.39

Table 2 summarizes the size of the absorption difference across the magnetically driven transition to the fully saturated state. Changes are largest in the low-frequency region in both systems. The ClO_4^- material also shows stronger distortions compared to the PF_6^- material. We find that $[\text{Cu}(\text{pyz})_2(2-\text{HOpy})_2](\text{PF}_6)_2$ and $[\text{Cu}(\text{pyz})_{1.5}(4-\text{HOpy})_2](\text{ClO}_4)_2$ undergo

Table 2. Summary of the Magnetoactive Vibrations in $[Cu(pyz)_2(2-HOpy)_2](PF_6)_2$ and $[Cu(pyz)_{1.5}(4-HOpy)_2](CIO_4)_2^a$

anion	mode position (cm^{-1})	assignment	$\Delta lpha/lpha \ (\%)$	$\Delta\omega$ (cm ⁻¹)	(cm^{-1})
PF ₆	472	o.o.p. pyz distance	25	0.48	1.9
	488	o.o.p. pyz distance	18	0.52	2.1
	797	C-H o.o.p. pyz distance	2	0.05	0.2
ClO ₄ ⁻	487	o.o.p. pyz distance	25	0.66	2.7
	489	o.o.p. pyz distance	33	0.73	2.9

"We show the percent changes of absorption across the quantum critical transition of these modes, along with field-induced frequency shifts and corresponding spin–phonon coupling constants. These are related as $\omega \approx \omega_0 + \lambda \langle S_i \cdot S_j \rangle$. Here, λ is the spin–phonon coupling constant. o.o.p. = out-of-plane.

somewhat different magnetically driven local lattice distortions because of their respective dimensionalities. At low temperature, the Cu^{2+} centers of the ladder have a tendency to form dimers, 46,47 causing the isolation of important exchange interactions. With an applied magnetic field, the mechanism required to fully saturate a pair of spins therefore depends, to a lesser extent, on distortions along the rails, and the effects are localized within the rungs. 48 In contrast, the distortion in $\mathrm{PF_6}^-$ is more complex, requiring a combination of out-of-plane pyz motions along multiple directions.

We can also extract frequency shifts $\Delta\omega$ across the magnetic quantum-phase transitions. Parts c and f of Figure 3 display the absolute value of the frequency shift $|\Delta\omega|$ along with 1.5 K magnetization ^{33,34} and the square of magnetization. We find that the field-induced frequency shifts follow $[M(B)]^2$, rising with increasing field and leveling off above the critical field, $B_{\rm C}$. This demonstrates that an applied field drives both systems into the fully saturated magnetic state ^{36,49} and that certain ligand-related phonons are sensitive to the change in spin state. A sharp knee—like that in the magnetization—is not observed at $B_{\rm C}$ because our magnetoinfrared measurements were taken slightly above the ordering temperatures. Nevertheless, shortrange interactions are sufficiently strong in both complexes to preserve the essential physics across the quantum-phase transition. ^{39,50}

Well-defined frequency shifts allow determination of the spin-phonon coupling constants across the magnetic quantum-phase transition. 51,52 Generally, these values are defined as $\omega = \omega_0 + \lambda \langle S_i \cdot S_i \rangle$, where ω_0 and ω are the unperturbed and perturbed phonon frequencies, $\langle S_i \cdot S_j \rangle$ is the nearest-neighbor spin-spin correlation function, and λ is the mode-dependent spin-phonon coupling constant. 53,54 At sufficiently low temperatures, the spin-spin correlation $\langle S_i \rangle$ S_i is $S^2 = (1/2)^2 = 1/4$ for Cu^{2+} spins. The magnitude of λ provides information about how the magnetic exchange interaction J is modulated by certain phonon displacements u because $\lambda = \partial^2 I/\partial u^2$. Therefore, by tracking the frequency shifts of the out-of-plane pyz vibrational modes in [Cu- $(pyz)_2(2-HOpy)_2](PF_6)_2$ and $[Cu(pyz)_{1.5}(4-HOpy)_2](ClO_4)_2$ across the magnetically driven transition to the fully saturated state, we can extract the spin-lattice coupling constants. Table 2 summarizes field-induced frequency shifts and the corresponding λ values for each field-dependent mode. In the following discussion, we focus on the out-of-plane pyz distortion near 490 cm⁻¹ because, in both cases, λ is large.

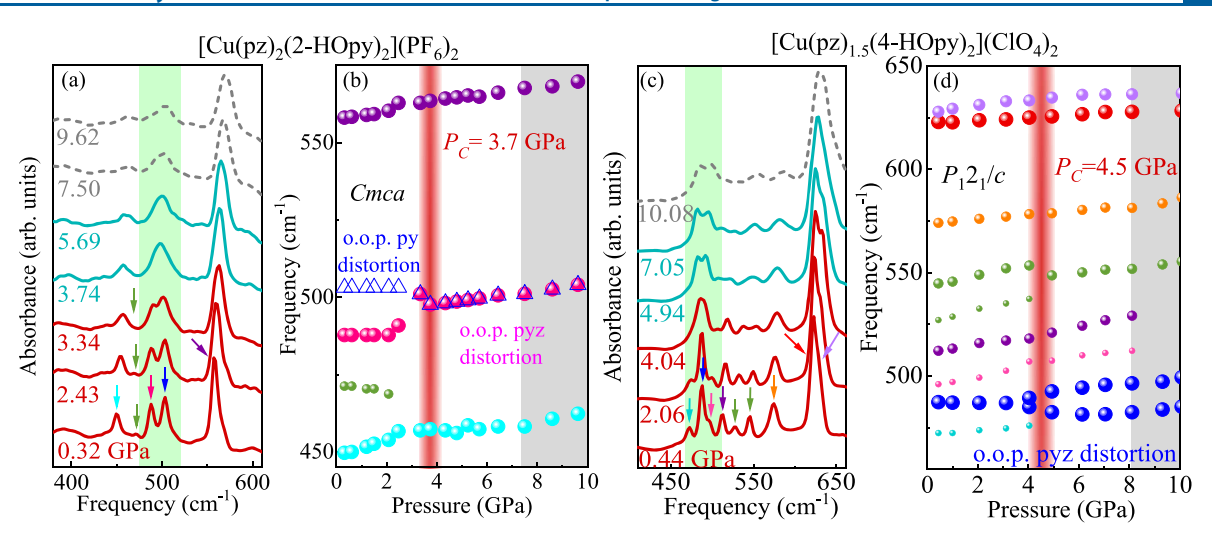


Figure 4. (a and c) Close-up views of the 300 K infrared spectra as a function of the pressure for $[Cu(pyz)_2(2-HOpy)_2](PF_6)_2$ and $[Cu(pyz)_{1.5}(4-HOpy)_2](ClO_4)_2$, respectively. The spectra are offset for clarity. The vertical green regions highlight pressure-driven distortions. (b and d) Frequency versus pressure trends for the modes displayed in parts a and c. Critical pressures P_C are indicated by vertical red lines. The gray areas indicate the point at which each system becomes amorphous (Supporting Information).

With the addition of $[Cu(pyz)_2(2-HOpy)_2](PF_6)_2$ and $[Cu(pyz)_{1.5}(4-HOpy)_2](ClO_4)_2$, the collection of coppercontaining coordination polymers for which λ values have been evaluated across the magnetic quantum-phase transition is now broad enough to allow several interesting structureproperty effects to emerge. Figure 3g summarizes the spinphonon coupling constants for the pyz bend in this class of materials.37-The overall trend is interesting. The pyz distortion in the spin ladder $[Cu(pyz)_{1.5}(4-HOpy)_{2}](ClO_{4})_{2}$ sports the strongest spin-phonon coupling ($\lambda = 2.9 \text{ cm}^{-1}$), whereas the one- and two-dimensional materials have slightly lower values ranging from 2.5 cm⁻¹ in the chain compound to between 1.2 and 2 cm⁻¹ in the various layered systems. This difference arises because of the unique structure of the spin ladder. In the quasi-two-dimensional materials, connectivity extends in the ab plane. In the quasi-one-dimensional systems, distortions occur primarily in the rail direction. Both systems require several local lattice distortions to facilitate the transition to the fully saturated spin state. What makes the ladder unique is the tendency toward low-temperature dimerization,⁴⁷ which, in $[Cu(pyz)_{1.5}(4-HOpy)_2](ClO_4)_2$, makes the pyz ligand the primary magnetic interaction pathway between Cu²⁺ centers in the rung. By undergoing an out-ofplane bend, a single local lattice distortion can reduce the antiferromagnetic part of *J* and stabilize the fully saturated spin state. 37,39

Pressure-Induced Structural Phase Transitions in Copper-Containing Coordination Polymers. Spin—lattice interactions can also be explored under compression. Sec. This is because pressure distorts the soft ligands that act as superexchange pathways in molecule-based magnetic materials and, by so doing, triggers changes in the magnetic states. Both processes can be probed spectroscopically. Parts a and c of Figure 4 display close-up views of the infrared responses of [Cu(pyz)₂(2-HOpy)₂](PF₆)₂ and [Cu(pyz)_{1.5}(4-HOpy)₂]-(ClO₄)₂ as a function of the pressure at 300 K. We only display results up to 10 GPa because, although not necessarily apparent in this energy window, both complexes become amorphous above 8 GPa (dashed gray lines). A detailed discussion is available in the Supporting Information. We focus on the behavior of the pyz- and py-related modes in order to

link our findings with the temperature and field effects. We track frequency versus pressure trends (Figure 4b,d) to quantify the pressure-driven spectral changes. Although inherently similar in composition, differences in the local structure and dimensionality drive these materials to unique high-pressure phases.

Parts a and b of Figure 4 summarize the vibrational properties of $[Cu(pyz)_2(2-HOpy)_2](PF_6)_2$ as a function of the pressure. The 487 cm⁻¹ out-of-plane pyz bend (which links the metal centers) hardens under compression, whereas the 503 cm⁻¹ py distortion (which stabilizes the layered structure) softens. The two branches come together across the 3.7 GPa structural phase transition (Figure 4b), consistent with the development of a higher-symmetry phase. The 450 and 470 cm⁻¹ modes (py- and pyz-containing distortions, respectively) converge across the critical pressure $P_{\rm C}$ as well. Naturally, the easy axis of compression in the PF₆⁻ compound is along c. Pressure therefore enhances the interlayer hydrogen bonding and stabilizes the structure. The py bending mode softens as a result, analogous to the aforementioned temperature trends (Figure 4b). The primary contraction along the c axis that strengthens interlayer interactions is accompanied by a relatively simple ab plane shrinkage that brings the Cu2+ centers closer together while distorting the pyz ligands.

The $[Cu(pyz)_{1.5}(4-HOpy)_2](ClO_4)_2$ spin ladder displays local lattice distortions that are consistent with a change in the symmetry under compression. Although many of the modes harden systematically under pressure, the out-of-plane pyz distortion at 487 cm⁻¹ splits across the 4.5 GPa transition (Figure 4d). Thus, while the pyz ligands in the rung and rail directions are nearly indistinguishable in the low-pressure phase, the system becomes anisotropic above $P_{\rm C}$ = 4.5 GPa. We anticipate strengthened Cu···Cu exchange pathways in the rung direction because of the natural tendency for spin ladders to dimerize.⁶⁰ Although pressure may improve interladder hydrogen bonding, these interactions, as in the temperature and magnetoinfrared measurements, are relatively weak. In any case, splitting of the out-of-plane pyz distortion across the pressure-driven transition in the ClO₄⁻ complex is consistent with the development of a lower-symmetry space group. A subgroup analysis of the $P2_1/c$ space group⁶¹ reveals several

candidate high-pressure phases including P1, $P2_1$, and P_C . In the $P2_1/c$ space group, an inversion center is present as a result of the intersection of a c-glide plane and a 2-fold screw axis (2_1) . The lower-symmetry space groups do not have this intersection. All of the potential low-symmetry structures including P1, $P2_1$, and P_C are therefore ferroelectric, 61 suggesting that low-dimensional magnetic materials like $[\mathrm{Cu}(\mathrm{pyz})_{1.5}(4\mathrm{-HOpy})_2](\mathrm{ClO}_4)_2$ have potential applications as multiferroics. The transition to a lower-symmetry space group along with pressure-induced modifications to the superexchange pathways may also shift the magnetic quantum-phase transition to lower fields. 25

Given the variety of copper-containing coordination polymers and the fact that spin-phonon coupling constants are sizable and show clear structure-property relationships across the magnetic quantum-phase transition (Figure 3g), we sought to correlate the behavior across P_{C} with magnetic dimensionality. There is, however, no apparent trend, probably because of the complexity of the pressure-induced transitions in these materials. In fact, many copper and nickel coordination complexes have multiple structural transitions under compression with signatures of disorder above 8 or 10 GPa. 62,63 While an applied field drives these materials into the fully saturated state in such a way that the field-dependent local lattice distortions modulate the superexchange pathway, pressure induces a more generalized lattice response with contributions from all of the soft linkages. Only a few of these trigger magnetic crossovers.

SUMMARY AND OUTLOOK

In this work, we combined vibrational spectroscopy with a number of different external stimuli to explore spin-lattice coupling in $[Cu(pyz)_2(2-HOpy)_2](PF_6)_2$ and $[Cu(pyz)_{1.5}(4-PV)_2](PF_6)_2$ $HOpy)_2$ (ClO₄)₂. The Cu centers in both systems are linked by pyz ligands, and by following the local lattice distortions under temperature, magnetic field, and pressure, we can analyze the magnetoelastic coupling. One of the most fascinating trends emerges across the magnetic quantumphase transition. While zero-dimensional (or "dot-like") systems connected only by intermolecular hydrogen bonds display no spin-lattice coupling across this type of field-driven transition, coupling increases in the one-dimensional case, reaches a maximum in the ladder, and falls again in layered analogues. The availability of a chemically related family of copper-containing quantum magnets including the ladder system, $[Cu(pyz)_{1.5}(4-HOpy)_2](ClO_4)_2$, is key to unveiling this trend. These findings are applicable to other classes of materials with field-induced transitions from the antiferromagnetic -> fully saturated state including molecule-based multiferroic and single-sheet analogues.^{64–6}

ASSOCIATED CONTENT

Supporting Information

The Supporting Information is available free of charge at https://pubs.acs.org/doi/10.1021/acs.inorgchem.9b02394.

Detailed explanation of the mode assignments and a discussion of the high-pressure, amorphous phase (PDF)

Accession Codes

CCDC 1515157 and 1553982 contain the supplementary crystallographic data for this paper. These data can be obtained free of charge via www.ccdc.cam.ac.uk/data_request/cif, or by

emailing data_request@ccdc.cam.ac.uk, or by contacting The Cambridge Crystallographic Data Centre, 12 Union Road, Cambridge CB2 1EZ, UK; fax: +44 1223 336033.

AUTHOR INFORMATION

Corresponding Author

Janice L. Musfeldt — Department of Chemistry and Department of Physics, University of Tennessee, Knoxville, Tennessee 37996, United States; orcid.org/0000-0002-6241-823X; Email: musfeldt@utk.edu

Authors

Kendall D. Hughey − Department of Chemistry, University of Tennessee, Knoxville, Tennessee 37996, United States; orcid.org/0000-0002-8501-5425

Nathan C. Harms – Department of Chemistry, University of Tennessee, Knoxville, Tennessee 37996, United States; orcid.org/0000-0002-2600-825X

Kenneth R. O'Neal – Department of Chemistry, University of Tennessee, Knoxville, Tennessee 37996, United States; orcid.org/0000-0001-9149-1957

Amanda J. Clune — Department of Chemistry, University of Tennessee, Knoxville, Tennessee 37996, United States; orcid.org/0000-0001-8618-1700

Jeffrey C. Monroe — Carlson School of Chemistry and Biochemistry, Clark University, Worcester, Massachusetts 01610, United States

Avery L. Blockmon — Department of Chemistry, University of Tennessee, Knoxville, Tennessee 37996, United States; orcid.org/0000-0002-0951-9832

Christopher P. Landee – Department of Physics, Clark University, Worcester, Massachusetts 01610, United States

Zhenxian Liu — Department of Civil and Environmental Engineering, Institute of Materials Science, The George Washington University, Washington, D.C. 20052, United States Mykhaylo Ozerov — National High Magnetic Field Laboratory, Tallahassee, Florida 32310, United States

Complete contact information is available at: https://pubs.acs.org/10.1021/acs.inorgchem.9b02394

Notes

The authors declare no competing financial interest.

ACKNOWLEDGMENTS

Research at the University of Tennessee is supported by the National Science Foundation (NSF; Grant DMR-1707846) and the Materials Research Fund. A portion of this work was performed at the National High Magnetic Field Laboratory, which is funded by National Science Foundation Cooperative Agreement DMR-1644779 and the State of Florida. Work at the National Synchrotron Light Source-II at Brookhaven National Laboratory is funded by the Department of Energy (DOE; Grant DE-AC98-06CH10886). Beamline 22-IR-1 is supported by COMPRES, the Consortium for Materials Properties Research in Earth Sciences, under NSF Cooperative Agreement EAR 1606856 and the DOE/National Nuclear Security Administration (Grant DE-NA-0003858; Centre for Development of Advanced Computing). We thank Mark Turnbull for useful discussions.

REFERENCES

(1) Zapf, V.; Jaime, M.; Batista, C. D. Bose–Einstein condensation in quantum magnets. *Rev. Mod. Phys.* **2014**, *86*, 563–614.

- (2) Vasiliev, A.; Volkova, O.; Zvereva, E.; Markina, M. Milestones of low-D quantum magnetism. *npj Quantum Mater.* **2018**, *3*, 18.
- (3) Zapf, V. S.; Correa, V. F.; Sengupta, P.; Batista, C. D.; Tsukamoto, M.; Kawashima, N.; Egan, P.; Pantea, C.; Migliori, A.; Betts, J. B.; Jaime, M.; Paduan-Filho, A. Direct measurement of spin correlations using magnetostriction. *Phys. Rev. B: Condens. Matter Mater. Phys.* 2008, 77, 020404.
- (4) Qin, W.; Xu, B.; Ren, S. An organic approach for nanostructured multiferroics. *Nanoscale* **2015**, *7*, 9122–9132.
- (5) Manson, J. L.; Huang, Q. Z.; Brown, C. M.; Lynn, J. W.; Stone, M. B.; Singleton, J.; Xiao, F. Magnetic structure and exchange interactions in quasi-one-dimensional MnCl₂(urea)₂. *Inorg. Chem.* **2015**, *54*, 11897–11905.
- (6) Hong, T.; Schmidt, K. P.; Coester, K.; Awwadi, F. F.; Turnbull, M. M.; Qiu, Y.; Rodriguez-Rivera, J. A.; Zhu, M.; Ke, X.; Aoyama, C. P.; Takano, Y.; Cao, H.; Tian, W.; Ma, J.; Custelcean, R.; Zhou, H. D.; Matsuda, M. Magnetic ordering induced by interladder coupling in the spin-1/2 Heisenberg two-leg ladder antiferromagnet C₉H₁₈N₂CuBr₄. *Phys. Rev. B: Condens. Matter Mater. Phys.* **2014**, 89, 174432.
- (7) Landee, C. P.; Turnbull, M. M. Recent developments in low-dimensional copper(II) molecular magnets. *Eur. J. Inorg. Chem.* **2013**, 2013, 2266.
- (8) O'Neal, K. R.; Lee, J. H.; Kim, M. S.; Manson, J. L.; Liu, Z.; Fishman, R. S.; Musfeldt, J. L. Competing magnetostructural phases in a semiclassical system. *npj Quantum Mater.* **2017**, *2*, 65.
- (9) Liu, J.; Kittaka, S.; Johnson, R. D.; Lancaster, T.; Singleton, J.; Sakakibara, T.; Kohama, Y.; Van Tol, J.; Ardavan, A.; Williams, B. H.; Blundell, S. J.; Manson, Z. E.; Manson, J. L.; Goddard, P. A. Unconventional field-induced spin gap in an S = 1/2 chiral staggered chain. *Phys. Rev. Lett.* **2019**, *122*, 057207.
- (10) Horiuchi, S.; Okimoto, Y.; Kumai, R.; Tokura, Y. Quantum phase transition in organic charge-transfer complexes. *Science* **2003**, 299, 229–232.
- (11) Gaita-Ariño, A.; Luis, F.; Hill, S.; Coronado, E. Molecular spins for quantum computation. *Nat. Chem.* **2019**, *11*, 301–309.
- (12) Sachdev, S.; Keimer, B. Quantum criticality. *Phys. Today* **2011**, 64, 29–35.
- (13) Blosser, D.; Bhartiya, V. K.; Voneshen, D. J.; Zheludev, A. z=2 quantum critical dynamics in a spin ladder. *Phys. Rev. Lett.* **2018**, *121*, 247201
- (14) Lancaster, T.; et al. Controlling magnetic order and quantum disorder in molecule-based magnets. *Phys. Rev. Lett.* **2014**, *112*, 207201.
- (15) Čižmár, E.; Ozerov, M.; Wosnitza, J.; Thielemann, B.; Krämer, K. W.; Rüegg, C.; Piovesana, O.; Klanjšek, M.; Horvatić, M.; Berthier, C.; Zvyagin, S. A. Anisotropy of magnetic interactions in the spinladder compound $(C_5H_{12}N)_2CuBr_4$. Phys. Rev. B: Condens. Matter Mater. Phys. **2010**, 82, 054431.
- (16) Stone, M. B.; Reich, D. H.; Broholm, C.; Lefmann, K.; Rischel, C.; Landee, C. P.; Turnbull, M. M. Extended quantum critical phase in a magnetized spin-1/2 antiferromagnetic chain. *Phys. Rev. Lett.* **2003**, *91*, 037205.
- (17) Validov, A. A.; Lavrentyeva, E. M.; Ozerov, M.; Zvyagin, S. A.; Turnbull, M. M.; Landee, C. P.; Teitel'baum, G. B. Quantum critical dynamics of S = 1/2 antiferromagnetic Heisenberg chains studied in CuPzN by ESR. J. Phys. Conf. Ser. 2010, 200, 022070.
- (18) Schlueter, J. A.; et al. Importance of halogen "halogen contacts for the structural and magnetic properties of CuX_2 (pyrazine- N_1N' -dioxide)(H_2O)₂ (X = Cl and Br). *Inorg. Chem.* **2012**, *51*, 2121–2129.
- (19) Awwadi, F. F.; Haddad, S. F.; Turnbull, M. M.; Landee, C. P.; Willett, R. D. Copper-halide bonds as magnetic tunnels; structural, magnetic and theoretical studies of trans-bis(2,5-dibromopyridine)-dihalo copper(II) and trans-bis(2-bromopyridine)dibromo copper-(II). CrystEngComm 2013, 15, 3111–3118.
- (20) Coleman, P.; Schofield, A. Quantum criticality. *Nature* **2005**, 433, 226–229.
- (21) Kono, Y.; Sakakibara, T.; Aoyama, C. P.; Hotta, C.; Turnbull, M. M.; Landee, C. P.; Takano, Y. Field-induced quantum criticality

- and universal temperature dependence of the magnetization of a spin-1/2 Heisenberg chain. *Phys. Rev. Lett.* **2015**, *114*, 037202.
- (22) Luo, Y.; Lu, X.; Dioguardi, A. P.; Rosa, P. S.; Bauer, E. D.; Si, Q.; Thompson, J. D. Unconventional and conventional quantum criticalities in CeRh_{0.58}Ir_{0.42}In₅. npj Quantum Mater. **2018**, *3*, 6.
- (23) Narumi, Y.; Terada, N.; Tanaka, Y.; Iwaki, M.; Katsumata, K.; Kindo, K.; Kageyama, H.; Ueda, Y.; Toyokawa, H.; Ishikawa, T.; Kitamura, H. Field induced lattice deformation in the quantum antiferromagnet SrCu₂(BO₃)₂. *J. Phys. Soc. Jpn.* **2009**, 78, 043702.
- (24) Zhao, L.; Fernández-Díaz, M. T.; Tjeng, L. H.; Komarek, A. C. Oxyhalides: a new class of high- T_C multiferroic materials. *Sci. Adv.* **2016**, 2, 1–5.
- (25) Ghannadzadeh, S.; Möller, J. S.; Goddard, P. A.; Lancaster, T.; Xiao, F.; Blundell, S. J.; Maisuradze, A.; Khasanov, R.; Manson, J. L.; Tozer, S. W.; Graf, D.; Schlueter, J. A. Evolution of magnetic interactions in a pressure-induced Jahn-Teller driven magnetic dimensionality switch. *Phys. Rev. B: Condens. Matter Mater. Phys.* 2013, 87, 241102.
- (26) Huddart, B. M.; Brambleby, J.; Lancaster, T.; Goddard, P. A.; Xiao, F.; Blundell, S. J.; Pratt, F. L.; Singleton, J.; Macchi, P.; Scatena, R.; Barton, A. M.; Manson, J. L. Magnetic order and enhanced exchange in the quasi-one-dimensional molecule-based antiferromagnet Cu(NO₃)₂(pyz)₃. *Phys. Chem. Chem. Phys.* **2019**, 21, 1014–1018. (27) Yu, J. H.; Xu, J. Q.; Ye, L.; Ding, H.; Jing, W. J.; Wang, T. G.; Xu, J. N.; Jia, H. B.; Mu, Z. C.; Yang, G. D. Hydrothermal synthesis and characterization of a copper(I) halide coordination polymer with isonicotinic acid (IN) ligand as a template possessing three-dimensional supramolecular network structure. *Inorg. Chem. Commun.* **2002**, *5*, 572–576.
- (28) Lapidus, S. H.; Manson, J. L.; Liu, J.; Smith, M. J.; Goddard, P.; Bendix, J.; Topping, C. V.; Singleton, J.; Dunmars, C.; Mitchell, J. F.; Schlueter, J. A. Quantifying magnetic exchange in doubly-bridged Cu- X_2 -Cu (X = F, Cl, Br) chains enabled by solid state synthesis of CuF₂(pyrazine). *Chem. Commun.* **2013**, *49*, 3558.
- (29) Ozerov, M.; Zvyagin, A. A.; Čižmár, E.; Wosnitza, J.; Feyerherm, R.; Xiao, F.; Landee, C. P.; Zvyagin, S. A. Spin dynamics in S = 1/2 chains with next-nearest-neighbor exchange interactions. *Phys. Rev. B: Condens. Matter Mater. Phys.* **2010**, 82, 014416.
- (30) Lanza, A.; Fiolka, C.; Fisch, M.; Casati, N.; Skoulatos, M.; Rüegg, C.; Krämer, K. W.; Macchi, P. New magnetic frameworks of $[(CuF_2(H_2O)_2)_x(pyz)]$. Chem. Commun. **2014**, 50, 14504.
- (31) Prescimone, A.; Morien, C.; Allan, D.; Schlueter, J. A.; Tozer, S. W.; Manson, J. L.; Parsons, S.; Brechin, E. K.; Hill, S. Pressure-driven orbital reorientations and coordination-sphere reconstructions in [CuF₂(H₂O)₂(pyz)]. *Angew. Chem., Int. Ed.* **2012**, *51*, 7490–7494.
- (32) Halder, G. J.; Chapman, K. W.; Schlueter, J. A.; Manson, J. L. Pressure-induced sequential orbital reorientation in a magnetic framework material. *Angew. Chem., Int. Ed.* **2011**, *50*, 419–421.
- (33) Landee, C. P.; Nizar, N.; Richardson, K.; Monroe, J. C.; Turnbull, M. M.; Polson, M.; Vela, S.; Blackmore, W.; Goddard, P. A.; Xiao, F.; Lancaster, T.; Williams, R. C.; Gape, P. M. D.; Pratt, F. L.; Blundell, S. J., unpublished work.
- (34) Landee, C. P.; Nizar, N.; Richardson, K.; Monroe, J. C.; Turnbull, M. M.; Polson, M.; Vela, S.; Blackmore, W.; Goddard, P. A.; Xiao, F.; Lancaster, T.; Williams, R. C.; Gape, P. M. D.; Pratt, F. L.; Blundell, S. J.; Dmytrileva, D.; Kuhne, H.; Ponomaryov, A.; Zvyagin, S., unpublished work.
- (35) Čižmăr, E.; Zvyagin, S. A.; Beyer, R.; Uhlarz, M.; Ozerov, M.; Skourski, Y.; Manson, J. L.; Schlueter, J. A.; Wosnitza, J. Magnetic properties of the quasi-two-dimensional S = 1/2 Heisenberg antiferromagnet [Cu(pyz)₂(HF₂)]PF₆. Phys. Rev. B: Condens. Matter Mater. Phys. **2010**, 81, 064422.
- (36) Goddard, P. A.; Singleton, J.; Sengupta, P.; McDonald, R. D.; Lancaster, T.; Blundell, S. J.; Pratt, F. L.; Cox, S.; Harrison, N.; Manson, J. L.; Southerland, H. I.; Schlueter, J. A. Experimentally determining the exchange parameters of quasi-two-dimensional Heisenberg magnets. *New J. Phys.* **2008**, *10*, 083025.
- (37) Günaydin-Şen, O.; Lee, Ć.; Tung, L. C.; Chen, P.; Turnbull, M. M.; Landee, C. P.; Wang, Y. J.; Whangbo, M.-H.; Musfeldt, J. L. Spin-

- lattice interactions through the quantum critical transition in Cu(pyz)(NO₃)₂. Phys. Rev. B: Condens. Matter Mater. Phys. **2010**, 81, 104307.
- (38) Al-Wahish, A.; O'Neal, K.; Lee, C.; Fan, S.; Hughey, K.; Yokosuk, M.; Clune, A.; Li, Z.; Schlueter, J.; Manson, J.; Whangbo, M.-H.; Musfeldt, J. Magnetic phase transitions and magnetoelastic coupling in S = 1/2 Heisenberg antiferromagnets. *Phys. Rev. B: Condens. Matter Mater. Phys.* **2017**, 95, 1–5.
- (39) Musfeldt, J. L.; Vergara, L. I.; Brinzari, T. V.; Lee, C.; Tung, L. C.; Kang, J.; Wang, Y. J.; Schlueter, J. A.; Manson, J. L.; Whangbo, M. H. Magnetoelastic coupling through the antiferromagnet-to-ferromagnet transition of quasi-two-dimensional [Cu(HF₂)(pyz)₂]BF₄ using infrared spectroscopy. *Phys. Rev. Lett.* **2009**, *103*, 147401.
- (40) Brinzari, T. V.; Chen, P.; Tung, L. C.; Kim, Y.; Smirnov, D.; Singleton, J.; Miller, J. S.; Musfeldt, J. L. Magnetoelastic coupling in [Ru₂(O₂CMe)₄]₃[Cr(CN)₆] molecule-based magnet. *Phys. Rev. B: Condens. Matter Mater. Phys.* **2012**, *86*, 214411.
- (41) Mao, H. K.; Xu, J.; Bell, P. M. Calibration of the ruby pressure gauge to 800 kbar under quasi-hydrostatic conditions. *J. Geophys. Res.* **1986**, *91*, 4673–4676.
- (42) Jones, B. R.; Varughese, P. A.; Olejniczak, I.; Pigos, J. M.; Musfeldt, J. L.; Landee, C. P.; Turnbull, M. M.; Carr, G. L. Vibrational properties of the one-dimensional, S=1/2, Heisenberg antiferromagnet copper pyrazine dinitrate. *Chem. Mater.* **2001**, *13*, 2127–2134.
- (43) Choi, J.; Woodward, J. D.; Musfeldt, J. L.; Landee, C. P.; Turnbull, M. M. Vibrational properties of $Cu(Pz)_2(ClO_4)_2$: Evidence for enhanced low-temperature hydrogen bonding in square S=1/2 molecular antiferromagnets. *Chem. Mater.* **2003**, *15*, 2797–2802.
- (44) Manson, J. L.; et al. Structural, electronic, and magnetic properties of quasi-1D quantum magnets $[Ni(HF_2)(pyz)_2]X$ (pyz = pyrazine; $X = PF_6$, SbF₆) exhibiting Ni-FHF-Ni and Ni-pyz-Ni spin interactions. *Inorg. Chem.* **2011**, *50*, 5990–6009.
- (45) Manson, J. L.; et al. Strong H···F hydrogen bonds as synthons in polymeric quantum magnets: structural, magnetic, and theoretical characterization of [Cu(HF₂)(pyrazine)₂]SbF₆, [Cu₂F(HF)(HF₂)-([yrazine)₄](SbF₆)₂, and [CuAg(H₃F₄)(pyrazine)₅](SbF₆)₂. *J. Am. Chem. Soc.* **2009**, *131*, 6733–6747.
- (46) Chaboussant, G.; Julien, M. H.; Fagot-Revurat, Y.; Hanson, M.; Lévy, L. P.; Berthier, C.; Horvatić, M.; Piovesana, O. Zero temperature phase transitions in spin-ladders: phase diagram and dynamical studies of $\text{Cu}_2(\text{C}_5\text{H}_{12}\text{N}_2)_2\text{Cl}_4$. Eur. Phys. J. B 1998, 6, 167–181.
- (47) Vaccarelli, O.; Rousse, G.; Saúl, A.; Radtke, G. Magnetic dimerization in the frustrated spin ladder $\text{Li}_2\text{Cu}_2\text{O}(\text{SO}_4)_2$. Phys. Rev. B: Condens. Matter Mater. Phys. **2017**, 96, 180406.
- (48) Bleaney, B.; Bowers, K. D. Anomalous paramagnetism of copper acetate. *Proc. R. Soc. London A* **1952**, 214, 451–465.
- (49) Granado, E.; García, A.; Sanjurjo, J. A.; Rettori, C.; Torriani, I.; Prado, F.; Sánchez, R. D.; Caneiro, A.; Oseroff, S. B. Magnetic ordering effects in the Raman spectra of La_{1-x}Mn_{1-x}O₃. *Phys. Rev. B: Condens. Matter Mater. Phys.* **1999**, *60*, 11879–11882.
- (50) De Jongh, L. J. Experiments on simple magnetic model systems. J. Appl. Phys. 1978, 49, 1305–1310.
- (51) Fennie, C. J.; Rabe, K. M. Magnetic and electric phase control in epitaxial EuTiO₃ from First Principles. *Phys. Rev. Lett.* **2006**, *97*, 267602.
- (52) Rudolf, T.; Kant, C.; Mayr, F.; Hemberger, J.; Tsurkan, V.; Loidl, A. Spin-phonon coupling in antiferromagnetic chromium spinels. *New J. Phys.* **2007**, *9*, 76.
- (53) Lee, J. H.; et al. A strong ferroelectric ferromagnet created by means of spin-lattice coupling. *Nature* **2010**, *466*, 954–958.
- (54) Sushkov, A. B.; Tchernyshyov, O.; Ratcliff, W., II; Cheong, S. W.; Drew, H. D. Probing spin correlations with phonons in the strongly frustrated magnet ZnCr₂O₄. *Phys. Rev. Lett.* **2005**, *94*, 137202.
- (55) Lee, J. H.; Rabe, K. M. Large spin-phonon coupling and magnetically induced phonon anisotropy in SrMO₃ perovskites

- (M=V,Cr,Mn,Fe,Co). Phys. Rev. B: Condens. Matter Mater. Phys. 2011, 84, 104440.
- (56) Zhuravlev, K. K.; Traikov, K.; Dong, Z.; Xie, S.; Song, Y.; Liu, Z. Raman and infrared spectroscopy of pyridine under high pressure. *Phys. Rev. B: Condens. Matter Mater. Phys.* **2010**, 82, 064116.
- (57) dela Cruz, C.; Yen, F.; Lorenz, B.; Wang, Y. Q.; Sun, Y. Y.; Gospodinov, M. M.; Chu, C. W. Strong spin-lattice coupling in multiferroic HoMnO₃: Thermal expansion anomalies and pressure effect. *Phys. Rev. B: Condens. Matter Mater. Phys.* **2005**, 71, 060407.
- (58) Saha, S.; Muthu, D. V.; Pascanut, C.; Dragoe, N.; Suryanarayanan, R.; Dhalenne, G.; Revcolevschi, A.; Karmakar, S.; Sharma, S. M.; Sood, A. K. High-pressure Raman and x-ray study of the spin-frustrated pyrochlore Gd₂Ti₂O₇. *Phys. Rev. B: Condens. Matter Mater. Phys.* **2006**, 74, 064109.
- (59) Wehinger, B.; et al. Giant pressure dependence and dimensionality switching in a metal-organic quantum antiferromagnet. *Phys. Rev. Lett.* **2018**, *121*, 117201.
- (60) Radtke, G.; Saúl, A.; Dabkowska, H. A.; Salamon, M. B.; Jaime, M. Magnetic nanopantograph in the $SrCu_2(BO_3)_2$ Shastry-Sutherland lattice. *Proc. Natl. Acad. Sci. U. S. A.* **2015**, *112*, 1971–1976.
- (61) Litvin, D. B. Ferroelectric Space Groups. Acta Crystallogr., Sect. A: Found. Crystallogr. 1986, A42, 44–47.
- (62) Musfeldt, J. L.; Liu, Z.; Li, S.; Kang, J.; Lee, C.; Jena, P.; Manson, J. L.; Schlueter, J. A.; Carr, G. L.; Whangbo, M.-H. Pressure-induced local structure distortions in Cu(pyz)F₂(H₂O)₂. *Inorg. Chem.* **2011**, *50*, 6347–6352.
- (63) O'Neal, K. R.; Holinsworth, B. S.; Chen, Z.; Peterson, P. K.; Carreiro, K. E.; Lee, C.; Manson, J. L.; Whangbo, M.-H.; Li, Z.; Liu, Z.; Musfeldt, J. L. Spin-lattice coupling in $[Ni(HF_2)(pyrazine)_2]SbF_6$ involving the HF_2^- superexchange pathway. *Inorg. Chem.* **2016**, *55*, 12172–12178.
- (64) Jain, P.; Ramachandran, V.; Clark, R. J.; Zhou, H. D.; Toby, B. H.; Dalal, N. S.; Kroto, H. W.; Cheetham, A. K. Multiferroic behavior associated with an order-disorder hydrogen bonding transition in metal-organic frameworks (MOFs) with the perovskite ABX₃ architecture. *J. Am. Chem. Soc.* **2009**, *131*, 13625–13627.
- (65) Ackermann, M.; Brüning, D.; Lorenz, T.; Becker, P.; Bohatý, L. Thermodynamic properties of the new multiferroic material (NH₄)₂[FeCl₅(H₂O)]. *New J. Phys.* **2013**, *15*, 123001.
- (66) Huang, C.; Du, Y.; Wu, H.; Xiang, H.; Deng, K.; Kan, E. Discovery of intrinsic ferromagnetic ferroelectricity in transition metal halides monolayer. *Phys. Rev. Lett.* **2018**, *120*, 147601.